ChemSystemsChem

Research Article
doi.org/10.1002/syst.202400094

Chemistry Europe
European Chemical Societies Publishing

www.chemsystemschem.org

Structural Screening of Short Peptide Amphiphiles with Autocatalytic Self-Replication

Ion Turcan[a, b] and Ignacio Insua*[a, b]

There is great interest in developing small synthetic molecules that imitate some of the functions and behaviour of living beings. Here, we describe the structural screening of peptide amphiphiles with autocatalytic self-replication, which mimics the perpetuation mechanisms of living matter. Our design uses two reactive precursors to generate self-assembling peptide amphiphiles, which form micelles that catalyse their own synthesis. A collection of precursors with varying sizes was screened combinatorially, revealing a minimal tripeptide amphiphile required to trigger autocatalytic self-replication. These results contribute to the structural simplification of synthetic supramolecular monomers with life-like behaviour.

Introduction

Molecular replication is a fundamental trait of living beings that allows the propagation of structural and functional information across generations. While specialised enzymes are required to replicate the genetic information of an organism,[1] other biomolecules like lipids and peptides are capable of autonomous molecular replication (*i.e.* self-replication).[2,3] In these cases, no enzyme is involved in the replicating process, instead, the self-assembly of the parent molecule into different structures (*e.g.* micelles, fibres, etc.) hosts the accumulation and/or templation of reactive precursors. This is an autocatalytic process, meaning that the self-replicating molecule catalyses the formation of molecular copies of itself by co-assembly with its precursors. For example, self-replicating amphiphiles can assemble micelles that favour the mixing and reactivity of immiscible precursors.[4,5] The self-replication of peptides has been engineered by hydrophobic interfacing of the parent peptide with two precursor fragments, both in α-helical[6] and β-sheet[7] conformations. Dynamic combinatorial libraries of peptides[8,9] or synthetic amphiphiles[10] allow the self-replication of a 'fitter' product from pools of competitors, mimicking Darwinian evolution by the spontaneous selection of a more favourable self-assembling product. Particularly interesting from an evolutionary standpoint are information-encoding self-replicators, like synthetic peptides[11,12] and nucleobase derivatives,[13,14] which can perpetuate structural information by the specific recognition of template sequences.[2,15]

The increasing interest in miniaturising functional assemblies from the bottom-up protocell and systems chemistry communities has fostered the design of small supramolecular monomers with cooperative behaviour, like self-replication. The challenge lies in reducing the size of a monomer to a minimum while retaining self-assembly and functional capacity. While small monomers are easy to produce and incorporate into other hybrid designs, their limited supramolecular contacts can compromise self-assembly affinity and specificity. In this context, peptides offer a versatile platform for the design of small supramolecular monomers with defined assembly modes and cooperative action. For example, the small fragment diphenylalanine is contained within the 42-amino acid sequence of the β-amyloid peptide, and it has been shown to self-assemble into nanofibres like its parent peptide.[16] Assemblies of histidine-containing octapeptides have shown esterase behaviour, similar to that found in the catalytic pockets of much larger enzyme structures.[17] These examples show the capacity of short peptides to mimic the structure and function of complex biomolecules through self-assembly.

Amongst all non-covalent interactions, hydrophobic packing tends to dominate supramolecular self-assembly in water. For this reason, peptides with conjugated aliphatic tails (*i.e.* peptide amphiphiles or lipopeptides) have been widely explored for nanomaterial assembly in biological and other aqueous media.[18] Just recently, peptide amphiphiles were shown to undergo autocatalytic self-replication for the first time.[19] However, while short peptide amphiphiles have been screened in self-assembly capacity with decreasing molecular size,[20,21] the miniaturisation of self-replicating peptide amphiphiles remains unexplored.

In this paper, we perform a systematic study of peptide amphiphile self-replication using progressively smaller molecules, aiming to identify the shortest peptide amphiphile capable of autocatalytic self-replication. A combination of spectroscopic, chromatographic and microscopy techniques confirmed the autocatalytic self-replication of a tripeptide in reaction with an aliphatic aldehyde, dodecanal, yielding cata-

[a] *Departamento de Farmacoloxía, Farmacia e Tecnoloxía Farmacéutica, Facultade de Farmacia, Universidade de Santiago de Compostela, Santiago de Compostela, Spain*

[b] *Current address: Centro Singular de Investigación en Química Biolóxica e Materiais Moleculares (CiQUS), Departamento de Farmacoloxía, Farmacia e Tecnoloxía Farmacéutica, Universidade de Santiago de Compostela, Santiago de Compostela, Spain*

***Correspondence:** Dr. Ignacio Insua, Departamento de Farmacoloxía, Farmacia e Tecnoloxía Farmacéutica, Facultade de Farmacia, Universidade de Santiago de Compostela, 15705, Santiago de Compostela, Spain.*
Email: ignacio.insua.lopez@usc.es

Supporting information for this article is available on the WWW under https://doi.org/10.1002/syst.202400094

lytic micelles not accessible from any shorter peptide amphiphile. The minimum structural requirements reported here for an autocatalytic self-replicating peptide amphiphile can be broadly applied to other functional supramolecular designs, contributing to the simplification of biomimetic assemblies and bottom-up protocell engineering.[22,23]

Results and Discussion

Peptide amphiphiles (PAs) are self-assembling monomers consisting of an aliphatic tail covalently attached to a peptide.[18] The peptide unit usually contains two regions: a hydrophobic β-sheet-inducing domain to promote self-assembly, and a charged end that provides colloidal stability to the final assembly. To engineer self-replicating behaviour in PAs, an efficient reaction is required to connect two PA precursors in the presence of their product as catalyst. One reported strategy to rapidly generate PAs in aqueous media is the connection of hydrophobic aldehydes to peptides bearing hydroxylamine groups, thus forming the oxime-connected PA products.[19,24,25] Based on these molecular designs, we decided to study the progressive reduction in size of PAs to identify the minimum structure required for autocatalytic self-replication.

A collection of four dormant (*i.e.* non-assembling) peptides, comprised of phenylalanine and glutamic acid residues as hydrophobic and charged domains respectively, were tested against three aliphatic aldehydes of varying length (Figure 1). The dormant peptides studied include a short dipeptide (**FE**), tripeptide ($\mathbf{F_2E}$), tetrapeptide ($\mathbf{F_2E_2}$) and pentapeptide ($\mathbf{F_3E_2}$). The hydroxylamine group at the N-terminus of these peptides would condensate with the reacting aldehydes ($\mathbf{T_8}$, $\mathbf{T_{10}}$ or $\mathbf{T_{12}}$) to afford a total of twelve combinatorial PA products. Each reaction product is denoted as the combined aldehyde and peptide codes (*e.g.* $\mathbf{T_{12}F_2E}$). Being formed in aqueous buffer, these PA products may self-assemble into micelles, which can catalyse the further connection of peptide and aldehyde precursors by accumulating these reactants at their amphiphilic interface (Figure 1 inset).

All peptides were synthesised on solid phase using methods previously reported[19,26] and characterised by NMR and HPLC-MS. The peptides were then combinatorially mixed with commercial aldehydes to assess their autocatalytic self-replication, using octanal ($\mathbf{T_8}$), decanal ($\mathbf{T_{10}}$) and dodecanal ($\mathbf{T_{12}}$) to evaluate the influence of longer -and hence more hydrophobic- aliphatic tails in the product PAs. Autocatalytic reactions are characterised by a sigmoidal kinetic profile, indicative of an isothermal acceleration of the reaction by the product formed, usually preceded by an induction phase (a.k.a. lag phase) where not enough product has yet been formed to trigger catalysis.[27] Induction phases to produce autocatalytic micelles can vary from a few minutes[10,19] to several hours[4,28] depending on precursor reactivity and product self-assembly (*i.e.* critical micelle concentration in a given medium). On this basis, we performed kinetic studies with all possible combinations of reactive peptides and aldehydes, looking for sigmoidal profiles indicative of an autocatalytic self-replication (Figure 2). In these experiments, peptide and aldehyde mixtures were incubated in the presence of the fluorescent probe thioflavin-T (ThT), which is a sensor for anionic micelles[29] and PA assemblies.[19,25] ThT emission was monitored over time as a reporter for the self-assembly of product PAs, providing insight into both the covalent connection of the precursors and the supramolecular association of the product, since the former is required for the latter. Like for other reported autocatalytic micelles,[28,30] reactions were stirred and heated, and reactive aldehydes were added from concentrated stocks in ethanol, all to maximise the solubility and mixing of reagents. We were pleased to find some sigmoidal profiles in the combinatorial screening of PA precursors (Figure 2). The longest peptide tested, $\mathbf{F_3E_2}$, showed two sigmoidal emission profiles, both with $\mathbf{T_{12}}$ and $\mathbf{T_{10}}$, while shorter $\mathbf{F_2E_2}$ and $\mathbf{F_2E}$ analogues only so with the longest aldehyde, $\mathbf{T_{12}}$. The two shortest precursors, **FE** and $\mathbf{T_8}$, did not show any indication of micellisation (*i.e.* ThT emission) in any of the combinations tested. These observations are consistent with larger and more hydrophobic PAs favouring self-assembly in water, unlike shorter and more polar PAs incapable of sufficient solvophobic packing. Interestingly, the shorter the

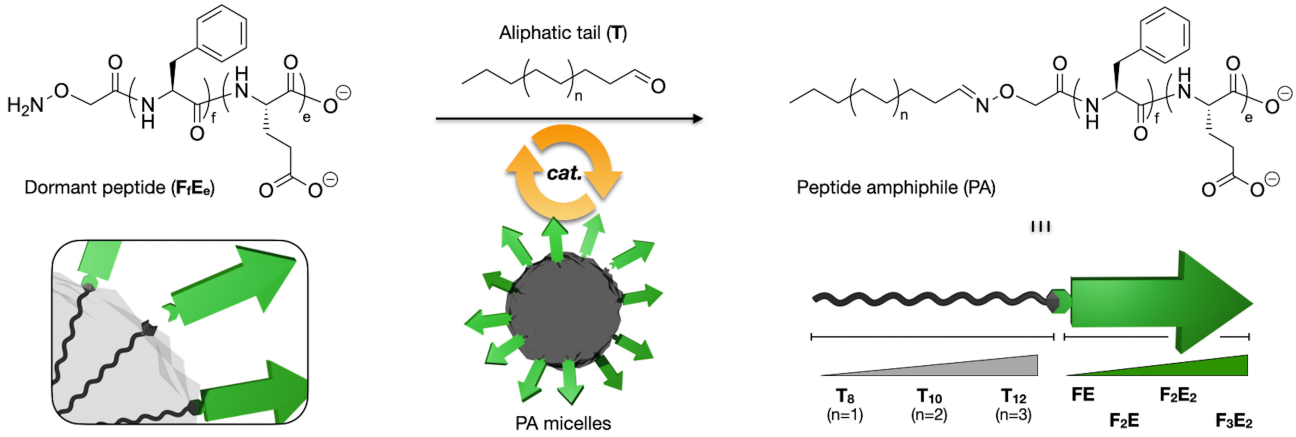

Figure 1. Reaction scheme of dormant non-assembling peptides with aliphatic aldehydes (*i.e.* tails) to generate peptide amphiphile (PA) products. PAs can self-assemble as micelles in the aqueous reaction medium, which can catalyse the further conversion of precursors into PAs by increasing the local concentration of reactive molecules at the amphiphilic surface of the micelles (bottom left inset).

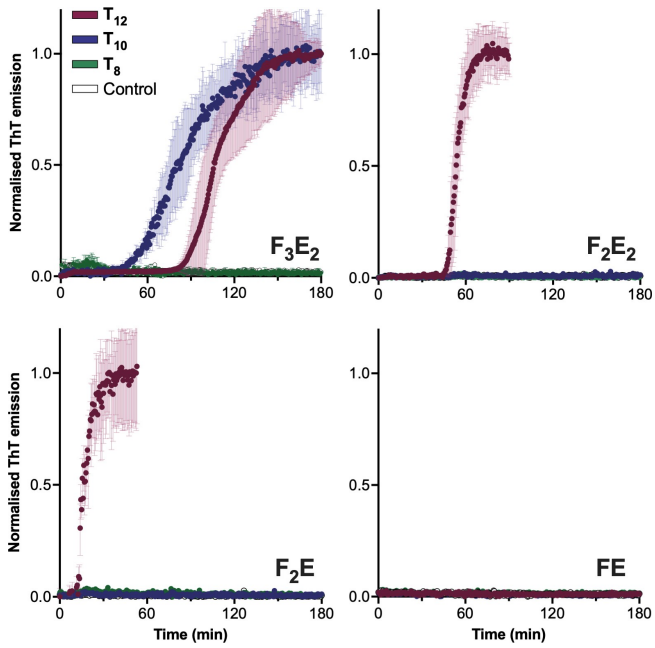

Figure 2. Thioflavin-T (ThT) emission kinetics of dormant peptide (F_3E_2, F_2E_2, F_2E and FE) and aldehyde tail (T_{12}, T_{10} and T_8) mixtures. Control samples were performed in the absence of aldehyde tail. Mean ± SD, $n = 3$.

peptide, the shorter the induction phase [**F_2E** (*ca.* 10 min) < **F_2E_2** (*ca.* 45 min) < **F_3E_2** (*ca.* 80 min) with **T_{12}**], which could result from the higher solubility and hence reactivity of shorter peptides. Overall, it was clear that **$T_{12}F_2E$** was the smallest PA structure tested to show a sigmoidal kinetic profile indicative of a potential autocatalytic self-replication.

To demonstrate the autocatalytic nature of **$T_{12}F_2E$** self-replication, seeding experiments were performed by doping a mixture of **T_{12}** and **F_2E** precursors with preformed PA product (Figure 3). Seeding assays involve the addition of product amphiphile at the start of the reaction, and demonstrate the autocatalytic nature of the process by reducing the induction phase.[19,31] Indeed, the presence of product **$T_{12}F_2E$** (*i.e.* seed) accelerated PA production and micellisation, shortening the induction time progressively with increasing **$T_{12}F_2E$** doping, from *ca.* 10 min without seeding to almost eliminating any induction phase at 10 mol% of seed.

Having identified **$T_{12}F_2E$** as the minimal autocatalytic self-replicating PA within the library studied, we set out to investigate the smaller analogue **$T_{12}FE$** to understand whether its lack of ThT signal (Figure 2) was due to a lack of covalent reactivity or supramolecular micellisation. Since ThT reports on the self-assembly of *in situ* generated PAs, we aimed to decouple the analysis of these two processes for a stepwise understanding. Firstly, HPLC-MS analysis of reaction mixtures confirmed the quantitative conversion of both **F_2E** and **FE** precursors into their corresponding **T_{12}** products (Figure 4A, MS spectra of HPLC peaks can be found in the supporting information). Secondly, the critical micelle concentration (CMC) of both PA products was studied spectroscopically, using Nile red as an environment-sensitive reporter for micelle formation.[32,33] The blueshift of Nile red's emission when this probe internalises in hydrophobic environments (*e.g.* micelle cores) was used to establish CMC values,[34] monitoring emission maxima at 655 and 633 nm as in-solution and in-micelle states, respectively (**Figure S1**). While the autocatalytic self-replicating **$T_{12}F_2E$** showed a CMC of 59 μM, consistent with the low μM range found for other PA CMCs,[19] **$T_{12}FE$** did not show any CMC transition in the range of concentrations tested (Figure 4B). Taken together, these results imply that while **FE** can efficiently react to form **$T_{12}FE$**, this PA product cannot form micelles in solution, setting a lower limit in the structural miniaturisation of PAs with assembly-driven autocatalytic self-replication.

The CMC found for **$T_{12}F_2E$** (59 μM) perfectly fits the results from the seeding experiments (Figure 3), where sub-CMC values of PA (*e.g.* 5 mol% = 50 μM) still require an induction time to generate catalytic micelles, whereas seed concentrations above the CMC (10 mol% = 100 μM) lack any induction time, having pre-formed micelles from the start of the experiment. These results show the autocatalytic nature of PAs is arising from their assembled micellar state, which can work as a nanoreactor that increases the local concentration of precursors and hence the reaction rate. It must be noted that *micellar autocatalysis*, also referred to as *physical autocatalysis*, is not a catalytic process in

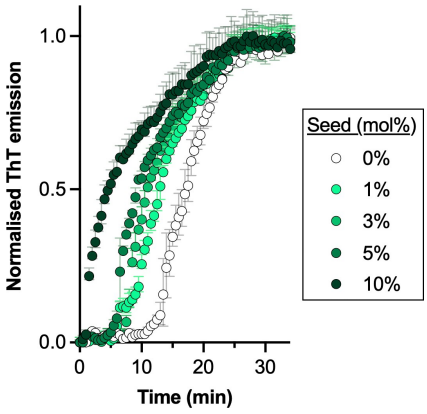

Figure 3. Thioflavin-T (ThT) emission kinetics of F_2E and T_{12} reaction mixtures in the presence of different amounts of their PA product, $T_{12}F_2E$ (seed). Mean ± SD, $n = 3$.

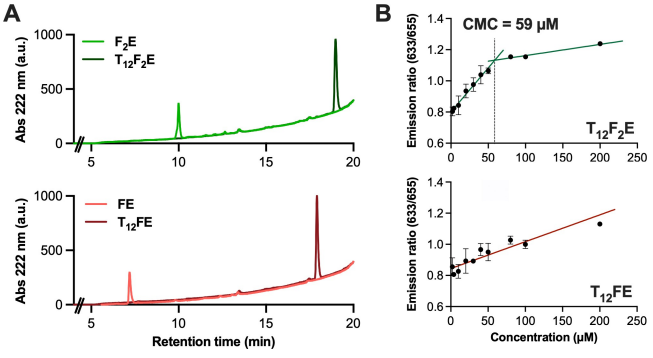

Figure 4. (A) Reverse-phase HPLC analysis of peptide precursors before (F_2E, FE) and 180 min after ($T_{12}F_2E$, $T_{12}FE$) the addition of reacting aldehyde T_{12}. (B) Critical micelle concentration (CMC) of PA products calculated by Nile red emission. Mean ± SD, $n = 3$.

strict terminology, as it does not decrease the activation energy of the reaction.[35] Instead, examples have shown that the solubilisation and mixing of amphiphile precursors within the micelles are responsible for the catalytic process.[36]

Finally, we decided to study the potential nanostructures formed by all $\mathbf{T_{12}}$ products, being this aldehyde the most hydrophobic one tested and hence the most likely to induce self-assembly. PAs can generate different nano-assemblies based on their molecular structure and assembly conditions (*e.g.* concentration, pH, etc.), mainly forming micelles and nanofibres.[18] Usually, the longer the peptide unit of the PA, the more favoured its linear propagation into nanofibres due to larger H-bond networks between peptide backbones. Unlike directional H-bonds, non-directional hydrophobic packing generally induces the micellisation of PAs with short peptide units. Mimicking the conditions of the kinetic studies (Figure 2), reaction mixtures of all four peptides with $\mathbf{T_{12}}$ were imaged by electron microscopy (Figure 5). Images showed that, while the two largest peptides, $\mathbf{F_3E_2}$ and $\mathbf{F_2E_2}$, both formed nanofibres with $\mathbf{T_{12}}$ -although the former in much higher amount-, $\mathbf{F_2E}$ only showed circular structures resemblant of micelles (ø = 65 ± 16 nm, **Figure S2**). Being analogous in amphiphilic core-shell structure, both micelles and nanofibres (a.k.a. cylindrical micelles)[37] can work as catalysts for the self-replication of their constituting PAs. Not surprisingly, the smallest peptide **FE** did not show any nanostructures by electron microscopy, confirming its inability to self-assemble, as suggested by all previous experiments. Dynamic light scattering confirmed the size of $\mathbf{T_{12}F_2E}$ micelles (D_H = 61 ± 11 nm, **Figure S3**), with all other samples producing larger structures, consistent with nanofibres of $\mathbf{T_{12}F_3E_2}$ and $\mathbf{T_{12}F_2E_2}$ and amorphous aggregates of $\mathbf{T_{12}FE}$. Importantly, the nanostructures found by STEM also demonstrate the negligible effect the reporters ThT and Nile red have on PA self-assembly -and hence autocatalysis-, since these probes are absent in electron microscopy samples (Figure 5).

Combined, our results demonstrate $\mathbf{T_{12}F_2E}$ is a true borderline autocatalytic PA size-wise, whose molecular structure is just amphiphilic enough to trigger micellar self-assembly, having any of the slight reductions in size tested (*i.e.* $\mathbf{T_{10}F_2E}$ or $\mathbf{T_{12}FE}$) fully compromise its self-assembling and autocatalytic behaviour.

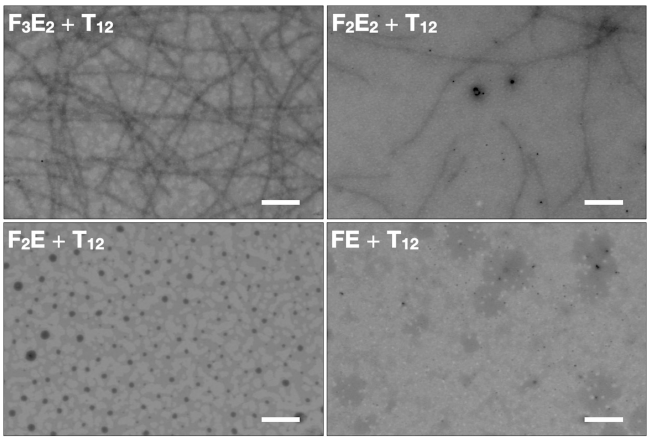

Figure 5. Representative scanning-transmission electron microscopy (STEM) images of all T_{12} reaction mixtures. Samples were stained with phosphotungstic acid. All scale bars = 400 nm.

Conclusions

We have identified $\mathbf{T_{12}F_2E}$ as a minimal autocatalytic self-replicating peptide amphiphile, capable of accelerating its own synthesis from two reactive precursors, $\mathbf{F_2E}$ and $\mathbf{T_{12}}$, through micellisation. Seeding experiments proved the autocatalytic nature of this process, with doping levels above $\mathbf{T_{12}F_2E}$'s CMC triggering catalysis from the start of the reaction (Figure 3, 10 mol%). The inability of the smaller $\mathbf{T_{12}FE}$ analogue to form catalytic micelles has been demonstrated with two self-assembly sensors, ThT (Figure 2) and Nile red (Figure 4B), and electron microscopy. Our results show a lower limit in the simplification of self-assembling PAs, not only for their autocatalytic self-replication, but also for their common assembly as nanofibres, not accessible from $\mathbf{T_{12}F_2E}$. We hope these results will guide future developments in functional biomimetic assemblies made from simple synthetic monomers, which can implement this minimal tripeptide amphiphile with autocatalytic self-replicating behaviour.

Experimental Methods

Solid-phase peptide synthesis. 2-chlorotrityl chloride resin (0.2-0.4 mmol) was reacted with the required Fmoc-protected amino acids (1.5 equiv.) in the presence of HBTU (1.3 equiv.) and DIPEA (4 equiv.) in DMF for 30 min. Fmoc deprotection was performed with 20 vol% piperidine in DMF for 30 min. After the final Fmoc deprotection, (Boc-aminooxy)acetic acid (8 equiv.) was coupled to the N-term of the peptide in the presence of DIC (8 equiv.) in DMF for 10 min. The resin was then cleaved with TFA:TIS:H_2O (95 : 2.5 : 2.5 vol%) for 2 h and the afforded solution precipitated into chilled diethyl ether, to then freeze-dry the pellet and thus isolate the peptides as white powders. All products were characterised by ^{1}H-NMR and HPLC-MS (see supporting information).

Peptide amphiphile synthesis. Peptides $\mathbf{F_2E}$ or **FE** (5 mg) were reacted with dodecanal ($\mathbf{T_{12}}$, 1.5 equiv.) in 1 mL of DMSO at 60 °C. After overnight incubation, the solutions were precipitated in acidic water and filtered. All products were characterised by HPLC-MS (see supporting information).

Kinetic study of PA formation and micellisation. Solutions of dormant peptide (1 mM) and ThT (250 μM) were prepared in 50 mM HEPES buffer pH 6.8, to which 5 μL of an aldehyde solution in ethanol (10 equiv.) were added to start the reaction. These reaction mixtures were prepared in triplicate to a final volume of 200 μL and fluorescence emission (ex = 485 nm, em = 520 nm) was measured every 30 s in a microplate reader at 40 °C with orbital shaking at 300 rpm (Figure 2). For data processing, all assembling samples (*i.e.* sigmoidal profiles) were normalised to their maximum emission, whereas flat kinetic profiles at baseline intensity were normalised to the maximum emission of the intermediate assembling PA, $\mathbf{T_{12}F_2E_2}$. Seeding experiments (Figure 3) were prepared and processed likewise, having different amounts (mol%) of preformed product $\mathbf{T_{12}F_2E}$ at the start of the reaction (*i.e.* before the addition of the aldehyde).

HPLC-MS analysis of precursor reactivity. Samples were prepared and incubated as indicated in the kinetic experiments above, only this time without ThT. **FE** and **F_2E** samples do not contain **T_{12}**, while **T_{12}FE** and **$T_{12}F_2$E** samples were analysed 180 min after the addition of **T_{12}** (Figure 4A). MS of all HPLC peaks can be found in the supporting information.

Critical micelle concentration (CMC) determination. For each sample, 10 μL of a 50 μM Nile red solution in acetone were left to dry overnight in an eppendorf tube protected from light. Next, 500 μL of serial dilutions of **$T_{12}F_2$E** and **T_{12}FE**, ranging from 2 to 200 μM in 50 mM HEPES buffer at pH 6.8, were added to these eppendorfs and samples were again incubated overnight in the dark. Each concentration was prepared in triplicate. The next day, samples were measured in a fluorimeter (ex = 550 nm, em = 570-700 nm) at 20 °C. The CMC was calculated as the crossing point between the two linear regimes found for Nile red's emission (Figure 4B).

Acknowledgements

This work was funded by the Agencia Estatal de Investigación (RYC2021-031367-I) and Xunta de Galicia (ED431F 2023/24, ED431 C 2024/09).

Conflict of Interests

The authors declare no conflict of interest.

Data Availability Statement

The data that support the findings of this study are available from the corresponding author upon reasonable request.

Keywords: self-assembly · peptide · supramolecular · autocatalysis · self-replication

[1] R. A. Ganai, E. Johansson, *Mol. Cell* **2016**, *62*, 745–755.
[2] P. Adamski, M. Eleveld, A. Sood, Á. Kun, A. Szilágyi, T. Czárán, E. Szathmáry, S. Otto, *Nat. Chem. Rev.* **2020**, *4*, 386–403.
[3] M. G. Howlett, S. P. Fletcher, *Nat. Chem. Rev.* **2023**, *7*, 673–691.
[4] I. Colomer, S. M. Morrow, S. P. Fletcher, *Nat. Commun.* **2018**, *9*, 2239.
[5] M. G. Howlett, A. H. J. Engwerda, R. J. H. Scanes, S. P. Fletcher, *Nat. Chem.* **2022**, *14*, 805–810.
[6] D. H. Lee, J. R. Granja, J. A. Martinez, K. Severin, M. R. Ghadiri, *Nature* **1996**, *382*, 525–528.
[7] B. Rubinov, N. Wagner, M. Matmor, O. Regev, N. Ashkenasy, G. Ashkenasy, *ACS Nano* **2012**, *6*, 7893–7901.
[8] F. Späth, H. Soria-Carrera, M. Stasi, J. Sastre, B. A. K. Kriebisch, J. Boekhoven, *Angew. Chem. Int. Ed.* **2024**, e202407424.
[9] J. W. Sadownik, E. Mattia, P. Nowak, S. Otto, *Nat. Chem.* **2016**, *8*, 264–269.
[10] R. Nguyen, L. Allouche, E. Buhler, N. Giuseppone, *Angew. Chem. Int. Ed.* **2009**, *48*, 1093–1096.
[11] O. Markovitch, J. Wu, S. Otto, *Angew. Chem. Int. Ed.* **2024**, *63*, e202317997.
[12] S. K. Rout, M. P. Friedmann, R. Riek, J. Greenwald, *Nat. Commun.* **2018**, *9*, 234.
[13] B. Liu, C. G. Pappas, J. Ottelé, G. Schaeffer, C. Jurissek, P. F. Pieters, M. Altay, I. Marić, M. C. A. Stuart, S. Otto, *J. Am. Chem. Soc.* **2020**, *142*, 4184–4192.
[14] T. A. Plöger, G. von Kiedrowski, *Org. Biomol. Chem.* **2014**, *12*, 6908–6914.
[15] T. Kosikova, D. Philp, *Chem. Soc. Rev.* **2017**, *46*, 7274–7305.
[16] S. Brahmachari, Z. A. Arnon, A. Frydman-Marom, E. Gazit, L. Adler-Abramovich, *ACS Nano* **2017**, *11*, 5960–5969.
[17] B. Sarkhel, A. Chatterjee, D. Das, *J. Am. Chem. Soc.* **2020**, *142*, 4098–4103.
[18] M. P. Hendricks, K. Sato, L. C. Palmer, S. I. Stupp, *Acc. Chem. Res.* **2017**, *50*, 2440–2448.
[19] R. Booth, I. Insua, S. Ahmed, A. Rioboo, J. Montenegro, *Nat. Commun.* **2021**, *12*, 6421.
[20] C. Vicente-Garcia, I. Colomer, *Nat. Chem. Rev.* **2023**, *7*, 710–731.
[21] R. Martí-Centelles, B. Escuder, *ChemNanoMat* **2018**, *4*, 796–800.
[22] K. P. Adamala, M. Dogterom, Y. Elani, P. Schwille, M. Takinoue, T.-Y. D. Tang, *Nat. Rev. Mol. Cell Biol.* **2024**, *25*, 162–167.
[23] I. Insua, J. Montenegro, *Chem* **2020**, *6*, 1652–1682.
[24] R. Kubota, K. Nagao, W. Tanaka, R. Matsumura, T. Aoyama, K. Urayama, I. Hamachi, *Nat. Commun.* **2020**, *11*, 4100.
[25] R. Booth, I. Insua, G. Bhak, J. Montenegro, *Org. Biomol. Chem.* **2019**, *17*, 1984–1991.
[26] C. Jiménez-Castells, B. G. De la Torre, R. G. Gallego, D. Andreu, *Bioorg. Med. Chem. Lett.* **2007**, *17*, 5155–5158.
[27] A. I. Hanopolskyi, V. A. Smaliak, A. I. Novichkov, S. N. Semenov, *ChemSystemsChem* **2021**, *3*, e2000026.
[28] P. A. Bachmann, P. L. Luisi, J. Lang, *Nature* **1992**, *357*, 57–59.
[29] S. Kumar, A. K. Singh, G. Krishnamoorthy, R. Swaminathan, *J. Fluoresc.* **2008**, *18*, 1199–1205.
[30] I. Budin, A. Debnath, J. W. Szostak, *J. Am. Chem. Soc.* **2012**, *134*, 20812–20819.
[31] A. J. Bissette, B. Odell, S. P. Fletcher, *Nat. Commun.* **2014**, *5*, 4607.
[32] Y. Shi, R. Lin, H. Cui, H. S. Azevedo, in *Biomaterials for Tissue Engineering: Methods and Protocols*, Springer Nature, **2018**, pp. 11–26.
[33] M. C. A. Stuart, J. C. Van de Pas, J. B. F. N. Engberts, *J. Phys. Org. Chem.* **2005**, *18*, 929–934.
[34] Y. Shi, D. S. Ferreira, J. Banerjee, A. R. Pickford, H. S. Azevedo, *Biomater. Sci.* **2019**, *7*, 5132–5142.
[35] A. J. Bissette, S. P. Fletcher, *Origins Life Evol. Biospheres* **2015**, *45*, 21–30.
[36] A. Kahana, D. Lancet, *Nat. Chem. Rev.* **2021**, *5*, 870–878.
[37] J. D. Hartgerink, E. Beniash, S. I. Stupp, *Science* **2001**, *294*, 1684–1688.

Manuscript received: November 26, 2024
Accepted manuscript online: January 9, 2025
Version of record online: January 20, 2025